ELSEVIER

Earth and Planetary Science Letters 186 (2001) 7–14

EPSL

www.elsevier.com/locate/epsl

A mantle plume below the Eifel volcanic fields, Germany

Joachim R.R. Ritter [a,*], Michael Jordan [a], Ulrich R. Christensen [a], Ulrich Achauer [b]

[a] *Institut für Geophysik, Universität Göttingen, Herzberger Landstr. 180, 37075 Göttingen, Germany*
[b] *Ecole et Observatiore des Sciences de la Terre, rue Rene Descartes 5, 67084 Strasbourg, France*

Received 25 September 2000; accepted 19 December 2000

Abstract

We present seismic images of the upper mantle below the Quaternary Eifel volcanic fields, Germany, determined by teleseismic travel time tomography. The data were measured at a dedicated network of more than 200 stations. Our results show a columnar low P-velocity anomaly in the upper mantle with a lateral contrast of up to 2%. The 100 km wide structure extends to at least 400 km depth and is equivalent to about 150–200 K excess temperature. This clear evidence for a plume below a region of comparatively minor volcanism suggests that deep mantle plumes could be more numerous than commonly assumed. They may often be associated with small volcanic fields or may have no volcanic surface expression at all.

Keywords: mantle plumes; hotspots; intraplate processes; volcanism; tomography

1. Introduction

Major hot-spots, centres of massive volcanism not linked to plate boundaries, such as Hawaii or Iceland, are commonly explained by mantle plumes [1]. These are believed to be 100–200 km wide columns of hot rock rising from great depth in the mantle that partially melt beneath the lithospheric plates. At a classical hot-spot, continuous magma production together with plate motion relative to the plume creates a hot-spot track, progressing in age away from the hot-spot. In contrast, for many intraplate volcanic centres with small eruption volumes and lack of a well-defined track, a plume-related origin is not clear. However, an extrapolation of the frequency–size distribution of observed hot-spots suggests that numerous smaller plumes may be present in the upper mantle [2] and may feed relatively small eruption centres. In the following we report results of a major seismic tomography experiment, addressing the mantle structure below the Eifel volcanic fields, Germany.

2. Setting

In the East and West Eifel volcanic fields in Germany, west of the river Rhine (Fig. 1), about 300 small eruptions occurred between 700 000 and 10 800 BP [3]. The total erupted volume of <15

* Corresponding author. Tel.: +49-551-397472; Fax: +49-551-397459; E-mail: ritter@uni-geophys.gwdg.de

0012-821X/01
PII: S0012-821X(01)00226-6

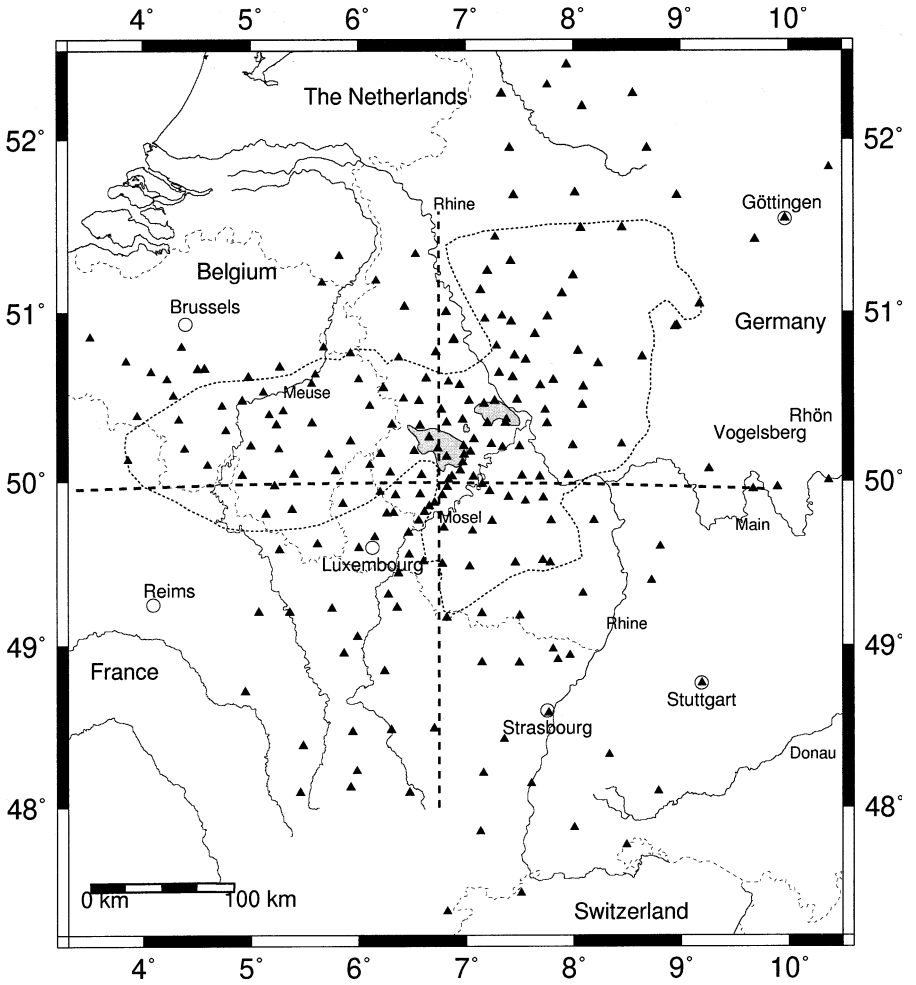

Fig. 1. Location map with seismic station distribution (triangles), volcanic fields in the Eifel region (in grey) and the outline of the Rhenish Massif (dotted curve). The two dashed lines indicate the positions of the cross-sections in Fig. 3.

km^3 represents an average magma flux that is several thousand times smaller than that of the Hawaiian hot-spot [4]. About 250 m of uplift in this time interval [5], ongoing exhalation of mantle helium [6], and isotopic and trace element signatures [7,8] all support a plume origin for the volcanism in the Eifel. It had been proposed that the various scattered volcanic fields (e.g. Vogelsberg, Rhön) stretching from the Eifel towards Eastern Europe represent a hot-spot track [9]. However, later radiometric dating [10] indicated that a clear age progression does not exist. As an alternative to a possible deep mantle origin it has been suggested that the Central European volcanism is related to the lithospheric stress field associated with the Alpine mountain building [11]. Earlier seismic studies indicated low velocities in the shallow mantle below the Eifel [12,13], but had no resolution below 200 km depth. A global tomography study shows a wide plume-like structure in the lower mantle below Central Europe [14], but no clear connection through the transition zone to the shallow mantle.

3. Methods and results

To image the mantle structure of the proposed

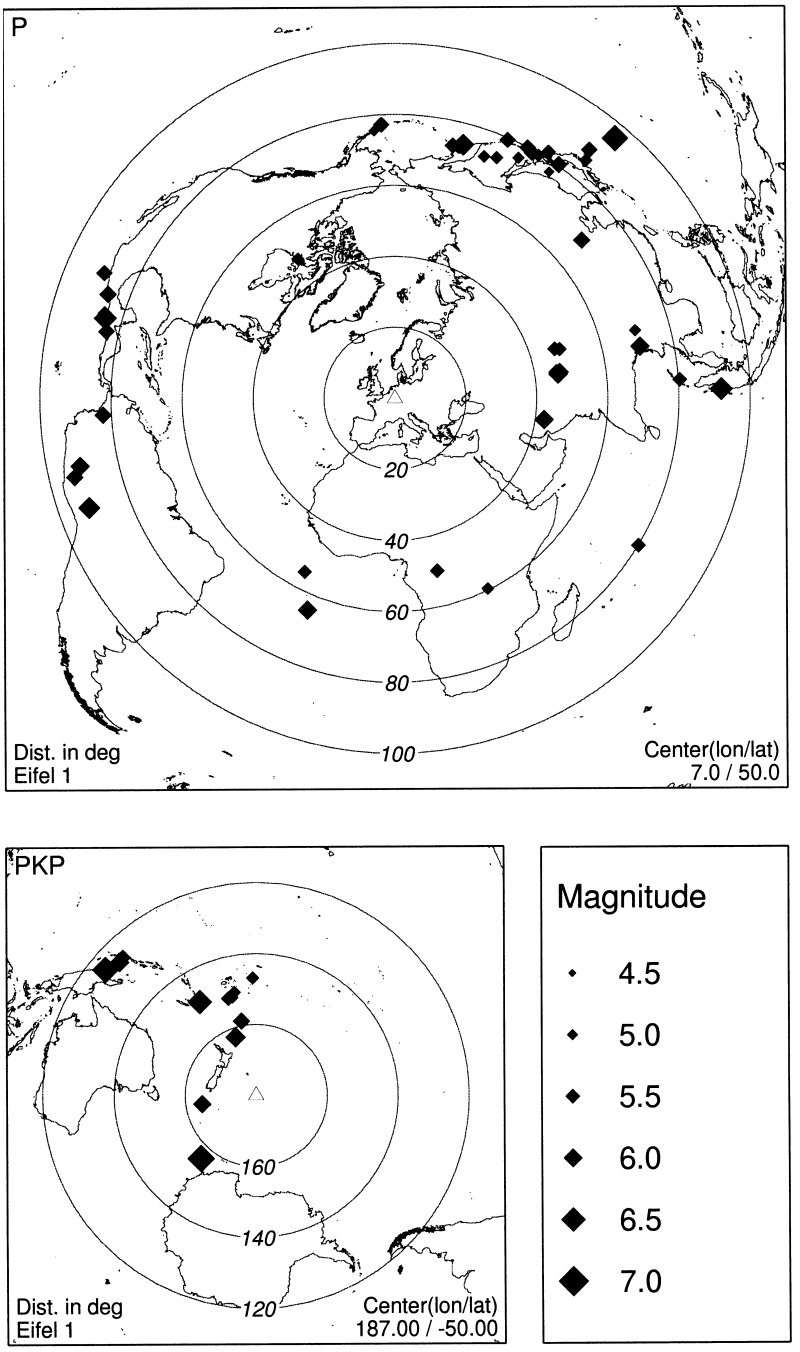

Fig. 2. Distribution of events. The distance is given in degrees relative to the centre of the station network (triangle). The data set contains travel time readings from 51 events with P as first arrival (upper map). The PKP arrivals are from 15 events with an epicentral distance of more than 120° (lower map). The body wave magnitude of the events ranges from about 4.9 to 6.8. Precise hypocentral parameters were taken from Engdahl et al. [33].

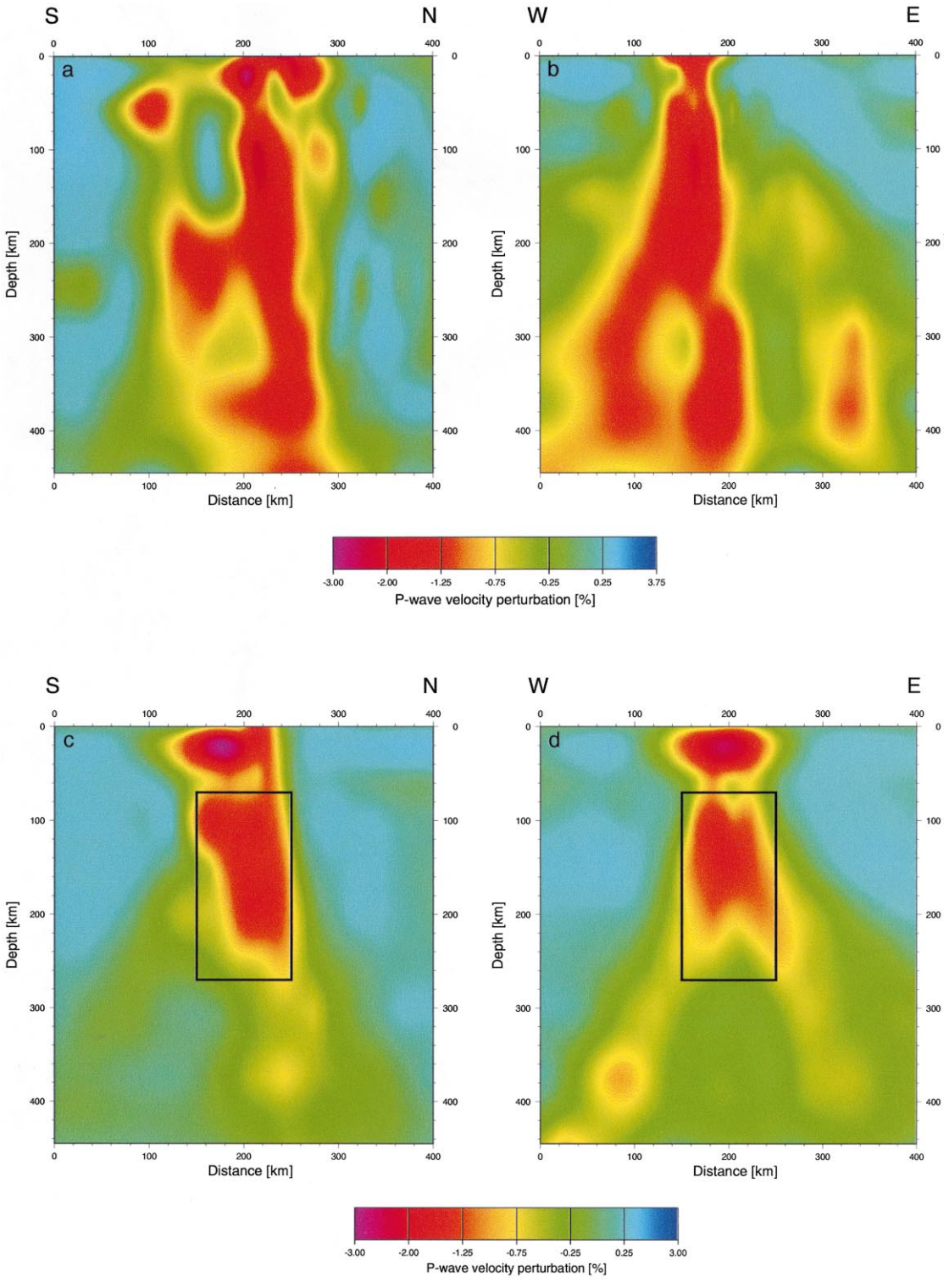
S
N
W
E
a
b
c
d
Depth [km]
Distance [km]
0
100
200
300
400
-3.00
-2.00
-1.25
-0.75
-0.25
0.25
3.75
3.00
P-wave velocity perturbation [%]

Fig. 3.

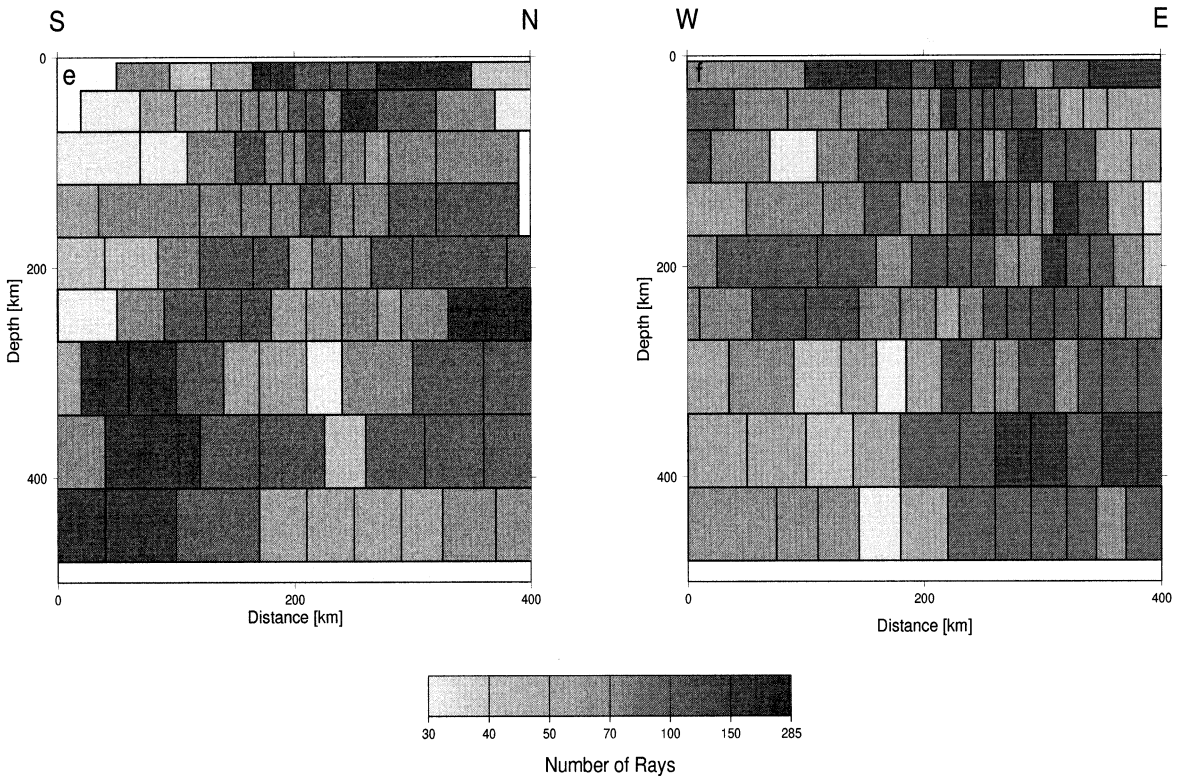

Fig. 3. Vertical cross-sections through the tomographic model. Displayed are perturbations of the P-wave velocity relative to the IASP91 model [16], on the sections indicated in Fig. 1. (a) S–N cross-section and (b) W–E cross-section. The reddish areas in the mantle are characterised by relatively low seismic velocity which most likely indicate increased temperature. (c) and (d) show reconstruction tests to estimate the effect of vertical smearing in the model space. As input structure, a 100 km wide synthetic plume from 70 to 270 km depth (outlined in black) with −3% velocity contrast is used. (e) and (f) display the block structure and ray coverage. Note that at least 30 rays with a good azimuthal coverage pass through each block.

Eifel plume with high resolution to a depth of at least 400 km, 10 European institutions operated a seismic network with an aperture of 500×500 km [15]. 158 mobile recording stations (Fig. 1) were deployed from November 1997 to June 1998. Data from 84 permanent stations add more observations of teleseismic waves. Details on the design of the network and instrument types are given in Ritter et al. [15]. To account for the different types of sensors, we deconvolved the instrument response functions. For a three-dimensional (3D) seismic tomography we determined 7319 P- and PKP-wave hand-picked arrival times with high precision at the restituted velocity seismograms. Based on the estimated accuracy of the timing, the data were sorted into three quality classes (±0.01 s, ±0.03 s and ±0.05 s) and were weighted accordingly in the inversion.

We achieve a good coverage of azimuths and ray parameters with 66 teleseismic events (Fig. 2). For our P-wave model we use 203 stations west of 10.5°E. P-wave travel time residuals are calculated by subtracting the theoretical travel time for the IASP91 [16] model from the observed travel time. To exclude travel time effects due to heterogeneities in the source region or event mislocation, we subtract the mean residual of each earthquake. This results in relative residuals that are mainly generated by seismic velocity perturbations underneath the station network. These relative residuals vary from −0.8 to +0.8 s at our stations. There is a clear regional trend for late arrivals near the

volcanic fields in the Eifel region, indicating reduced seismic velocity at depth.

To map the seismic velocity variations in the mantle a 3D tomographic inversion is used similar to Weiland et al. [17]. We include an uneven parameterisation depending on ray density and angular distribution of rays [18], resulting in 20–200 km wide blocks in 10 layers down to 480 km depth. The inversion algorithm is a Bayesian scheme accounting for data quality [19]. The starting model is equivalent to the 1D IASP91 [16] velocity distribution. The uppermost layer at 0–5 km depth with low seismic velocity (5.1 km/s) serves mainly to account for station statics. The resulting 3D velocity model explains 88.6% of the measured relative travel time residuals. In Fig. 3a,b we present perturbations of the compressional wave speed relative to the IASP91 model [16] for two vertical cross-sections (S–N and W–E). The point of intersection of the cross-sections corresponds approximately to the centre of the main anomaly. Velocity perturbations larger than about 0.5% are significant as found in resolution analyses (see Section 4). A clear low-velocity anomaly (LVA) from about 70 km to at least 400 km depth is found, centred slightly southwest of the West Eifel volcanic field. The width of this anomaly is about 100 km on average, and the velocity contrast to the surrounding mantle reaches up to 2%. Structure below 410 km depth is not well resolved, and the LVA may extend further down into the transition zone.

4. Resolution

Fig. 3e,f show the model parameterisation and ray density along the cross-sections. There are at least 30 rays per block with an adequate azimuthal coverage (Fig. 2). We performed reconstruction tests [20] to estimate the spatial resolution in the model space. Synthetic travel time residuals were calculated for various assumed velocity structures and for the ray geometry of the actual experiment. Then we inverted the synthetic data after adding Gaussian noise. Fig. 3c,d show an example in which we want to test whether the deep plume structure seen in Fig. 3a,b is true or the result of vertical smearing, along the ray paths, of a shallow low-velocity structure. The synthetic plume is 100 km wide, extends from 70 to 270 km depth and has a seismic velocity contrast of −3%. The recovered images in Fig. 3c,d are close to the input structure with only minor smearing of the velocity perturbations along the steeply inclined ray paths. The bottom of the synthetic plume at 270 km depth is blurred, however, a depth resolution of about 50 km can be achieved, suggesting that the deep plume structure seen in Fig. 3a,b has been reliably mapped. Checkerboard and spike tests confirm that velocity anomalies of ±2% and about 50 km lateral extent can be recovered in the upper mantle below the centre of the station network with our dataset. The largest artefact in our synthetic test is found at shallow depths above the plume (Fig. 3c,d). Because the teleseismic ray paths hardly cross at crustal depths, the upper 30 km are poorly resolved. Therefore, the low velocities at shallow depths in Fig. 3a,b might represent crustal heterogeneities, but they may be also artefacts of the inversion method.

5. Discussion and conclusions

The LVA in the upper mantle under the SW Eifel region is presumably caused by elevated temperature, because large P-velocity perturbations due to compositional variations are unlikely [21]. Accounting for first-order effects like anharmonicity [22,23] and anelasticity [21,24], the amplitude of the LVA underneath the Eifel can be explained by an excess temperature of 150–200 K (±100 K). The width of the anomaly and the inferred excess temperature agree approximately with estimates for plume conduits in the upper mantle from geodynamic and petrological models [25,26]. The temperature anomaly of the Eifel plume is similar to estimates based on seismic data for the plumes underneath the Massif Central (150–200 K) [21] and Iceland (about 150 K) [27], but is lower than for Hawaii (250–300 K) [28]. In seismic tomography the amplitude of anomalies is often reduced by smearing of structure. Because of the much higher station density than in comparable studies,

our result is probably less affected, which could imply that the maximum temperature anomaly might be slightly lower for the Eifel than it is for other plumes.

The main implication of our result is that even small intra-continental volcanic fields can draw their magma supply from much more voluminous upflows, rising from greater depth in the mantle. The melt production in the plumes is controlled by variations in buoyancy flux, volatile content, thickness of the overlying lithosphere and excess temperature of the plume [4,25,26,29]. Subtle differences in the last two parameters can have a strong influence on the magma generation rate. A slightly reduced plume temperature or thicker lithosphere can make a plume appear insignificant or entirely invisible in terms of magmatism.

A common source for the two currently active European upper-mantle plumes (Massif Central and Eifel) and possibly for other Tertiary volcanic fields in Europe could be the broad anomaly (500×500 km^2) in the lower mantle that has been identified with global tomography [14]. Convection modelling has shown that the endothermic phase boundary at 660 km depth could hold up a lower-mantle upwelling [30] with ponding of plume material in a broad reservoir in the transition zone, from where several narrow plumes could be launched through the upper mantle. Although a connection of the Eifel plume through the transition zone is not yet proven, testing such a model is a challenge for future investigations.

Acknowledgements

We thank S. Goes and an anonymous reviewer for useful comments. The following institutions were involved in the operation of the seismic network: GeoForschungsZentrum Potsdam, GeoZentrum Vulkaneifel, European Institute for Geodynamics and Seismology, Geological Survey of Nordrhein-Westfalen, Royal Observatory of Belgium and the Universities of Bochum, Cologne, Göttingen, Potsdam and Strasbourg. Further data were provided by Bundesanstalt für Geowissenschaften und Rohstoffe; Geological Survey Baden-Württemberg; ORFEUS data centre and Réseau National de Surveillance Sismique. A. Barth, M. Keyser, R. Meyer and M. Portmann helped with the data analysis. Seismic processing was done using SeismicHandler [31] and plotting was done with GMT [32]. This work was supported by the Deutsche Forschungsgemeinschaft (Ch77/9).*[AC]*

References

[1] W.J. Morgan, Convection plumes in the lower mantle, Nature 230 (1971) 42–43.
[2] B.D. Malamud, D.L. Turcotte, How many plumes are there?, Earth Planet. Sci. Lett. 174 (1999) 113–124.
[3] H.-U. Schmincke, V. Lorenz, H.A. Seck, The Quaternary Eifel volcanic fields, in: Fuchs et al. (Eds.), Plateau Uplift, Springer, Berlin, 1983, pp. 139–151.
[4] R.S. White, Melt production rates in mantle plumes, Philos. Trans. R. Soc. Lond. A 342 (1993) 137–153.
[5] W. Meyer, J. Stets, Junge Tektonik im Rheinischen Schiefergebirge und ihre Quantifizierung, Z. Dtsch. Geol. Ges. 149 (1998) 359–379.
[6] E. Griesshaber, R.K. O'Nions, E.R. Oxburgh, Helium and carbon isotope systematics in crustal fluids from the Eifel, the Rhine Graben and Black Forest, FRG, Chem. Geol. 99 (1992) 213–235.
[7] K. Hoernle, Y.-S. Zhang, D. Graham, Seismic and geochemical evidence for large-scale mantle upwelling beneath the eastern Atlantic and western and central Europe, Nature 374 (1995) 34–39.
[8] K.H. Wedepohl, A. Baumann, Central European Cenozoic plume volcanism with OIB characteristics and indications of a lower mantle source, Contrib. Miner. Petrol. 136 (1999) 225–239.
[9] R.A. Duncan, N. Petersen, R.B. Hargraves, Mantle plumes, movement of the European plate, and polar wandering, Nature 239 (1972) 82–85.
[10] H.J. Lippolt, Distribution of volcanic activity in space and time, in: Fuchs et al. (Eds.), Plateau Uplift, Springer, Berlin, 1983, pp. 112–120.
[11] K. Regenauer-Lieb, Dilatant plasticity applied to the Alpine collision: ductile void growth in the intraplate area beneath the Eifel volcanic field, J. Geodyn. 27 (1998) 1–21.
[12] S. Raikes, K.-P. Bonjer, Large-scale mantle heterogeneity beneath the Rhenish Massif and its vicinity from teleseismic P-residuals measurements, in: Fuchs et al. (Eds.), Plateau Uplift, Springer, Berlin, 1983, pp. 315–331.
[13] M.L. Passier, R.K. Snieder, Correlation between shear wave upper mantle structure and tectonic surface expressions: application to central and southern Germany, J. Geophys. Res. 101 (1996) 25293–25304.
[14] S. Goes, W. Spakman, H. Bijwaard, A lower mantle

source for Central European volcanism, Science 286 (1999) 1928–1931.
[15] J.R.R. Ritter, U. Achauer, U.R. Christensen The Eifel Plume Team,, The teleseismic tomography experiment in the Eifel region, Central Europe: design and first results, Seism. Res. Lett. 71 (2000) 437–443.
[16] B.L.N. Kennett, E.R. Engdahl, Travel times for global earthquake location and phase identification, Geophys. J. Int. 105 (1991) 429–465.
[17] C.M. Weiland, L.K. Steck, P.B. Dawson, V.A. Korneev, Nonlinear teleseismic tomography at Long Valley caldera, using three-dimensional minimum travel time ray tracing, J. Geophys. Res. 100 (1995) 20379–20390.
[18] W. Spakman, H. Bijwaard, Irregular cell parameterization of tomographic problems, Ann. Geophys. 16 (1998) 28.
[19] H. Zeyen, U. Achauer, Joint inversion of teleseismic delay times and gravity anomaly data for regional structures, in: K. Fuchs (Ed.), Upper Mantle Heterogeneities from Active and Passive Seismology, Kluwer Academic Publishers, Dordrecht, 1997, pp. 155–169.
[20] R.D. van der Hilst, E.R. Engdahl, W. Spakman, Tomographic inversion of P and pP data for aspherical mantle structure below the northwest Pacific region, Geophys. J. Int. 115 (1993) 264–302.
[21] S.V. Sobolev et al., Upper mantle temperatures and lithosphere–asthenosphere system beneath the French Massif Central constrained by seismic, gravity, petrologic and thermal observations, Tectonophysics 275 (1997) 143–164.
[22] O.L. Anderson, D. Isaak, H. Oda, High-temperature elastic constant data on minerals relevant to geophysics, Rev. Geophys. 30 (1992) 57–90.
[23] T.S. Duffy, D.L. Anderson, Seismic velocities in mantle minerals and the mineralogy of the upper mantle, J. Geophys. Res. 94 (1989) 1895–1912.
[24] S.-i. Karato, Importance of anelasticity in the interpretation of seismic tomography, Geophys. Res. Lett. 20 (1993) 1623–1626.
[25] R.S. White, D. McKenzie, Mantle plumes and flood basalts, J. Geophys. Res. 100 (1995) 17543–17585.
[26] N.M. Ribe, U.R. Christensen, The dynamical origin of Hawaiian volcanism, Earth. Planet. Sci. Lett. 171 (1999) 517–531.
[27] Y. Shen, S.C. Solomon, I.T. Bjarnason, C.J. Wolfe, Seismic evidence for a lower-mantle origin of the Iceland plume, Nature 395 (1998) 62–65.
[28] X. Li, R. Kind, K. Priestley, S.V. Sobolev, F. Tilmann, X. Yuan, M. Weber, Mapping the Hawaiian plume conduit with converted seismic waves, Nature 405 (2000) 938–941.
[29] M. Albers, U.R. Christensen, The excess temperature of plumes rising from the core–mantle boundary, Geophys. Res. Lett. 23 (1996) 3567–3570.
[30] D. Brunet, D.A. Yuen, Mantle plumes pinched in the transition zone, Earth Planet. Sci. Lett. 178 (2000) 13–27.
[31] K. Stammler, SeismicHandler: programmable multichannel data handler for interactive and automatic processing of seismological analyses, Comp. Geosci. 19 (1993) 135–140.
[32] P. Wessel, W.H.F. Smith, New, improved version of Generic Mapping Tools released, EOS Trans. Am. Geophys. Union 79 (1998) 579.
[33] E.R. Engdahl, R. van der Hilst, R. Buland, Global teleseismic earthquake relocation with improved travel times and procedures for depth determination, Bull. Seism. Soc. Am. 88 (1998) 722–743.